

Testing the strong equivalence principle with multimessenger binary neutron star mergers

Jie Zhu^{1†}, Hanlin Song^{2*†}, Zhenwei Lyu^{3*}, Hao Li^{1*}, Peixiang Ji², Jun-Chen Wang²,
Haobo Yan², Bo-Qiang Ma^{4,2*}

¹Department of Physics and Chongqing Key Laboratory for Strongly Coupled Physics, Chongqing University, Chongqing, 401331, China.

²School of Physics, Peking University, Beijing, 100871, China.

³Leicester International Institute, Dalian University of Technology, Panjin, 124221, China.

⁴School of Physics, Zhengzhou University, Zhengzhou, 450001, China.

*Corresponding author(s). E-mail(s): hanlin@stu.pku.edu.cn; zwlyu@dlut.edu.cn; haolee@cqu.edu.cn; mabq@pku.edu.cn;

†These authors contributed equally to this work.

Abstract

The constancy of the gravitational constant G is a cornerstone of the strong equivalence principle and of general relativity, yet its possible temporal variation remains a key target in tests of fundamental physics. Gravitational-wave (GW) astronomy, especially when combined with electromagnetic observations, provides an unprecedented new opportunity to probe this principle in the strong-field and dynamical regime. In this work, we develop a GW waveform model with a slowly varying gravitational constant, incorporating its effects both on compact binary dynamics and GW propagation in an expanding universe. Applying this framework to the binary neutron star merger GW170817, together with independent electromagnetic constraints on the luminosity distance, sky localization and binary inclination from GRB 170817A, we perform a joint Bayesian analysis that disentangles varying- G effects from astrophysical degeneracies. We find no evidence for a temporal variation of the gravitational constant, and constrain its fractional time derivative to $\dot{G}/G \in [-3.36 \times 10^{-9}, 5.34 \times 10^{-10}] \text{ yr}^{-1}$, representing the most stringent bounds obtained to date from real GW observations. Our results demonstrate the power of multi-messenger astronomy as a precision probe of the strong equivalence principle in the relativistic regime.

Einstein's theory of general relativity (GR) is one of the pillars of modern physics and has passed a wide range of experimental tests to date with remarkable precision, from the Solar System to astrophysical and cosmological scales [1–4]. Among its foundational principles, the strong equivalence principle (SEP) plays a central role: it states that all local nongravitational and gravitational experiments, including those involving gravitational self-energy, are independent of the location, velocity, and composition of the freely falling reference frame. A direct consequence of the SEP is the constancy of Newton's gravitational constant G . While the SEP has been stringently tested using lunar laser ranging, pulsar timing, the cosmic microwave background, and other observations [5–12], most existing constraints probe weak-field or quasi-static regimes. Testing the SEP in the strong-field, highly dynamical regime therefore remains an important open challenge.

The advent of gravitational-wave (GW) astronomy has opened a new window on gravity in precisely this regime. In particular, the binary neutron star (BNS) merger GW170817, detected by Advanced LIGO and Advanced Virgo on August 17, 2017 [13], marked the first observation of compact-object coalescence through both gravitational and electromagnetic channels. The detection of the associated short gamma-ray burst GRB 170817A just 1.7 seconds after the merger [14], followed by extensive multiwavelength follow-up observations [15], provided independent measurements of the sky localization, luminosity distance, and orbital inclination of the source [16–20]. This combination of GW and electromagnetic information enables a genuine multimessenger test of gravity, breaking key parameter degeneracies inherent to GW-only analyses and allowing for precision probes of fundamental principles in the strong-field and dynamical regime.

In this work, we exploit multimessenger observations of BNS coalescences to test the strong equivalence principle through a possible temporal variation of the gravitational constant. A slowly varying G provides a well-motivated and generic parameterization of SEP violation, with observable consequences for both the generation of GWs at the source and their propagation across cosmological distances. At the source, a time-dependent G modifies the dynamics of compact binaries through its correction to gravitational self-energy, leading to characteristic imprints on the inspiral phase evolution. These effects can be described in terms of object-dependent sensitivities [21], which quantify the response of compact objects to variations in G . At the same time, a varying gravitational constant alters the propagation of GWs in an expanding Friedmann–Lemaître–Robertson–Walker (FLRW) universe, inducing additional modifications to the observed waveform amplitude. A consistent test of the SEP therefore requires a framework that simultaneously accounts for both source and propagation effects.

Building on this framework, we implement a physically consistent GW waveform model that incorporates both source and propagation effects of a slowly varying gravitational constant, while enforcing equation-of-state (EOS) dependent mass bounds through compact-object sensitivities. We apply this framework to GW170817 and perform a joint Bayesian analysis that combines GW data with independent electromagnetic constraints from the GRB 170817A counterpart. We find no evidence for a temporal variation of the gravitational constant and constrain its fractional time derivative to $\dot{G}/G \in [-3.36 \times 10^{-9}, 5.34 \times 10^{-10}] \text{ yr}^{-1}$. These constraints, derived from real multimessenger observations, provide a controlled strong-field test of the SEP using compact binary mergers.

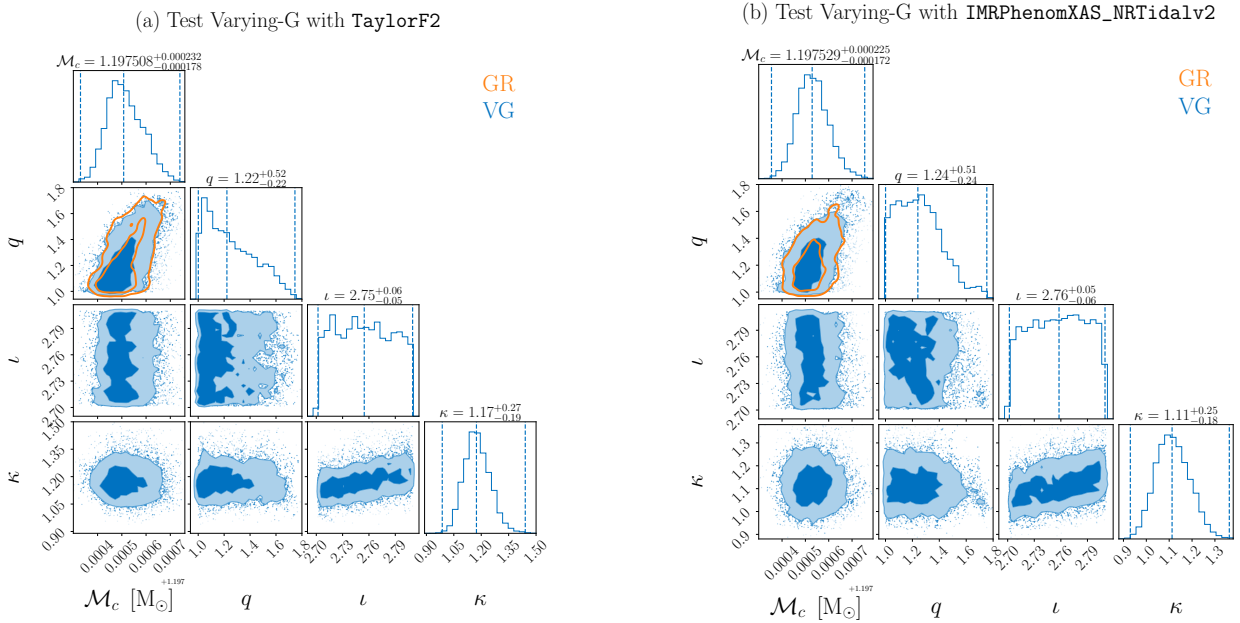


Fig. 1 Posterior distributions from multimessenger constraints on a varying gravitational constant. Posterior distributions of the key parameters are inferred from GW170817 using the TaylorF2 (left) and IMRPhenomXAS_NRTidalv2 (right) waveform models. The two-dimensional contours show the 50% and 90% credible regions, while the vertical lines indicate the 3σ intervals of the one-dimensional marginalized posteriors. Results obtained under GR are shown in orange, and those obtained within the varying- G framework are shown in blue.

Results and discussion

We analyze GW170817 strain data from LIGO Hanford and Livingston detectors, obtained from the Gravitational Wave Open Science Center (GWOSC) [22]. The data are processed with a low-frequency cutoff of 20 Hz and a reference frequency of 40 Hz. Bayesian parameter inference is performed using the PyCBC framework [23]. To ensure the robustness of our results, we employ two baseline GR waveform models, TaylorF2 and IMRPhenomXAS_NRTidalv2. Although the observed signal is dominated by the inspiral phase, merger–ringdown effects are also incorporated through a continuous (C^0) extension within IMRPhenomXAS_NRTidalv2 [24, 25]. In the Bayesian analysis, we incorporate independent electromagnetic constraints on the sky localization, luminosity distance, and orbital inclination of GW170817 [16–20], enabling a genuine multimessenger inference that breaks key degeneracies inherent to GW–only analyses.

The posterior distributions of the key parameters are shown in Fig. 1. The left and right panels present the results obtained with the TaylorF2 and IMRPhenomXAS_NRTidalv2 waveforms, respectively. In both cases, the GR posteriors for the chirp mass \mathcal{M}_c and mass ratio q are highlighted in orange. The inferred values of \mathcal{M}_c and q are consistent across waveform models and agree with previously reported results [26].

The corresponding posteriors obtained within the varying- G framework are shown in blue. For both waveform families, the inferred values of \mathcal{M}_c , q , and the remaining intrinsic and extrinsic parameters remain fully consistent with their GR counterparts. No statistically significant shift is observed between the GR and varying- G analyses, nor between

the two waveform models, indicating that the posterior distributions are stable against both modeling choices and the inclusion of a varying gravitational constant.

The non-GR parameter $\kappa = G_*/G_0$, which quantifies the ratio of the gravitational constant at the source to that measured at the detector, is constrained to $\kappa = 1.17_{-0.19}^{+0.27}$ and $\kappa = 1.11_{-0.18}^{+0.25}$ (3σ credible intervals) using the TaylorF2 and IMRPhenomXAS.NRTidalv2 waveforms, respectively. The close agreement between these independent waveform models further supports the robustness of the inferred constraints. Using the lookback time of GW170817, these results translate into bounds on the temporal variation of the gravitational constant of $[-3.36 \times 10^{-9}, 1.53 \times 10^{-10}] \text{ yr}^{-1}$ and $[-2.75 \times 10^{-9}, 5.34 \times 10^{-10}] \text{ yr}^{-1}$, respectively. Adopting a conservative interpretation, we obtain a combined 3σ constraint of \dot{G}/G of $[-3.36 \times 10^{-9}, 5.34 \times 10^{-10}] \text{ yr}^{-1}$. It is instructive to compare our results with previous GW-based studies that constrain a possible temporal variation of the gravitational constant [27–36]. Early analyses based on Fisher-matrix techniques and Monte Carlo simulations for GW151226, which incorporated both amplitude and phase corrections within the parametrized post-Einsteinian framework, yielded comparatively weak bounds of $|\dot{G}/G| \lesssim 2.20 \times 10^4 \text{ yr}^{-1}$ [29]. Subsequent work constrained \dot{G}/G by imposing physically allowed neutron-star mass ranges, derived from the Tolman–Oppenheimer–Volkoff (TOV) equations, on the projected GR mass posteriors of GW170817, obtaining bounds at the level of $\dot{G}/G \sim [-7 \times 10^{-9}, 5 \times 10^{-8}] \text{ yr}^{-1}$ [30]. Other studies exploited varying- G effects on GW propagation, using projected GR luminosity distance posteriors of GW170817 to infer constraints of order $|\dot{G}/G| \lesssim 10^{-9} \text{ yr}^{-1}$ [33, 34, 36].

By contrast, our analysis performs a full Bayesian inference using the observed GW170817 data, incorporating independent electromagnetic constraints on the source geometry and distance, while simultaneously accounting for both source-generation and propagation effects of a varying gravitational constant and enforcing neutron-star mass bounds derived from TOV equations. This approach improves upon earlier Fisher-matrix estimates and confirms, with real multimessenger data, the projected constraints inferred from GR posteriors of GW170817.

In summary, we present a comprehensive multimessenger analysis that constrains a possible temporal variation of the gravitational constant as a test of the SEP. We find no evidence for a temporal variation of G , and place a conservative 3σ bound of $\dot{G}/G \in [-3.36 \times 10^{-9}, 5.34 \times 10^{-10}] \text{ yr}^{-1}$, representing the most stringent constraints obtained to date from real GW observations.

Related physics in varying- G theory

Modified GW waveform templates in varying- G theory

To model the impact of a time-varying gravitational constant on GW signals, we adopt the parametrized post-Einsteinian (ppE) framework [28, 37]. In the frequency domain, the ppE waveform for a compact binary inspiral can be written as [37]

$$\tilde{h}(f) = \tilde{h}_{\text{GR}}(f) (1 + \alpha u^a) e^{i\beta u^b}, \quad (1)$$

where $\tilde{h}_{\text{GR}}(f)$ denotes the GR waveform. The terms αu^a and $\delta\Psi = \beta u^b$ represent non-GR corrections to the waveform amplitude and phase, respectively. Here $u \equiv (\pi \mathcal{M}_c f)^{1/3}$, with $\mathcal{M}_c \equiv (m_1 m_2)^{3/5} / (m_1 + m_2)^{1/5}$ the chirp mass defined in terms of the component masses m_1 and m_2 , and f the GW frequency. Deviations from GR are fully characterized by the ppE parameters $\{\alpha, \beta, a, b\}$. The explicit form of the ppE corrections induced by a varying gravitational constant was derived in Ref. [28]; here we briefly summarize the key physical ingredients relevant for our analysis.

In varying- G theories, the gravitational self-energy of a compact object depends explicitly on the gravitational constant. As a result, the mass of a body becomes time dependent when G varies in time. This induces an anomalous acceleration for a compact object moving with velocity \mathbf{v} in the cosmic frame, which in turn affects the orbital angular momentum of a binary system [21]. The response of a compact object to a variation in G is quantified by its sensitivity,

$$s = -\frac{G}{m} \frac{\delta m}{\delta G} = -\frac{\delta \ln m}{\delta \ln G}. \quad (2)$$

The anomalous acceleration \mathbf{a} can be then written as [21]

$$\mathbf{a} = s \frac{\dot{G}}{G} \mathbf{v}, \quad (3)$$

where the overdot denotes a derivative with respect to time. For a binary system with total mass denoted as $M = m_1 + m_2$ and total angular momentum denoted as j , the time evolution of these quantities induced by a varying- G is given by [21]

$$\dot{M} = -\frac{m_1 s_1 + m_2 s_2}{m_1 + m_2} \frac{\dot{G}}{G} M, \quad (4)$$

$$\dot{j} = \frac{m_1 s_1 + m_2 s_2}{m_1 + m_2} \frac{\dot{G}}{G} j, \quad (5)$$

where $j = \sqrt{GM}r$ and r denotes the binary separation. The combined variation of the total mass, gravitational constant, and angular momentum modifies the orbital separation at a rate

$$\dot{r}_{\dot{G}} = -\left(\frac{\dot{G}}{G} + \frac{\dot{M}}{M} - 2\frac{\dot{j}}{j}\right)r. \quad (6)$$

The full evolution of the binary separation is therefore

$$\dot{r} = \dot{r}_{\text{GW}} + \dot{r}_{\dot{G}}, \quad (7)$$

where the contribution from GW emission is

$$\dot{r}_{\text{GW}} = -\frac{64}{5} \frac{G^3 \mu M^2}{r^3}, \quad (8)$$

with $\mu = m_1 m_2 / M$ the reduced mass. Using the modified orbital evolution in Eq. (7), the ppE phase parameters associated with a varying gravitational constant are obtained as [28]

$$b = -13, \quad (9)$$

$$\beta = -\frac{25}{851968} \eta^{3/5} \frac{\dot{G}}{G} [(11 + 3(s_1 + s_2))GM - 41(Gm_1 s_1 + Gm_2 s_2)], \quad (10)$$

while the corresponding ppE amplitude parameters are [28]

$$a = -8, \quad (11)$$

$$\alpha = \frac{5}{512} \eta^{3/5} \frac{\dot{G}}{G} [(-7 + s_1 + s_2)GM + 13(Gm_1 s_1 + Gm_2 s_2)], \quad (12)$$

where $\eta = m_1 m_2 / M^2$ is the symmetric mass ratio. In this framework, the parameter of primary interest is the fractional time variation of the gravitational constant, \dot{G}/G , which we constrain using GW observations.

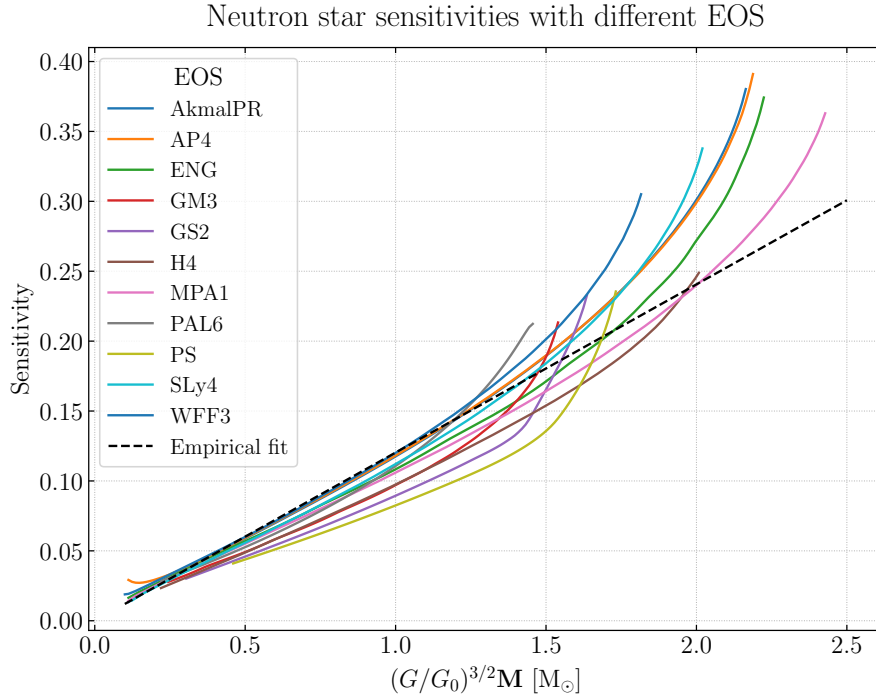


Fig. 2 Neutron-star sensitivities as a function of mass and gravitational constant for different equations of state. Neutron-star sensitivities are computed for several representative equations of state. The black dashed line shows the empirical relation given in Ref. [11, 38], while the colored curves correspond to sensitivities obtained from numerical solutions of the TOV equations. The EOSs are taken from Ref. [39].

Sensitivities for neutron stars

To construct the GW waveform templates in a theory with a time-varying gravitational constant, it is necessary to evaluate the sensitivities of compact objects. In previous GW-based studies of varying- G theories, the sensitivities of neutron stars

have often been estimated using the empirical relation from Refs [11, 38]. In this approach, the sensitivity is assumed to scale linearly with the neutron-star mass and is given by

$$s = 0.16 \left(\frac{\mathbf{M}}{1.33 \mathbf{M}_\odot} \right), \quad (13)$$

where \mathbf{M} denotes the neutron-star mass and \mathbf{M}_\odot is the solar mass. While this prescription provides a useful approximation, a more accurate determination of the sensitivity requires a self-consistent treatment based on the neutron-star EOS. Below we outline a numerical procedure to compute neutron-star sensitivities by solving the TOV equations for a given EOS.

Because any realistic temporal variation of G is expected to be small on timescales relevant to neutron-star structure, its direct contribution to the field equations can be neglected. The internal structure of neutron stars can therefore be described by the standard TOV equations, which read as follows

$$\begin{aligned} \frac{dm(r)}{dr} &= 4\pi r^2 \rho(r), \\ \frac{d\bar{m}_b(r)}{dr} &= 4\pi r^2 \epsilon_b(r) \left(1 - \frac{2Gm(r)}{r} \right)^{-1/2}, \\ \frac{dP(r)}{dr} &= - \frac{Gm(r)\rho(r)}{r^2} \left(1 + \frac{P(r)}{\rho(r)} \right) \left(1 + \frac{4\pi r^3 P(r)}{m(r)} \right) \left(1 - \frac{2Gm(r)}{r} \right)^{-1}, \end{aligned} \quad (14)$$

where $m(r)$ and $\bar{m}_b(r)$ denote the gravitational mass and the baryon mass enclosed by a radius r , respectively, and $P(r)$, $\rho(r)$ and $\epsilon_b(r)$ are the pressure, density and rest mass density at r . Given an EOS specifying the relations among $P(r)$, $\rho(r)$, and $\epsilon_b(r)$, and the center density $\rho(0) = \rho_c$, solving Eq. (14) yields the neutron-star radius R , gravitational mass $\mathbf{M} = m(R)$, and baryon mass $\bar{\mathbf{M}} = \bar{m}_b(R)$. We assume the baryon number is conserved in the varying- G scenario, such that the baryon mass of a neutron star remains unchanged under variations of G .

The G -dependence of Eq. (14) can be removed by introducing the rescaled variables

$$\begin{aligned} m &= G^{-\frac{3}{2}} m^*, \\ \bar{m}_b &= G^{-\frac{3}{2}} \bar{m}_b^*, \\ r &= G^{-\frac{1}{2}} r^*, \end{aligned} \quad (15)$$

in terms of which the TOV equations become

$$\begin{aligned} \frac{dm^*}{dr^*} &= 4\pi r^{*2} \rho, \\ \frac{d\bar{m}_b^*}{dr^*} &= 4\pi r^{*2} \epsilon_b \left(1 - \frac{2m^*}{r^*} \right)^{-1/2}, \\ \frac{dP}{dr^*} &= - \frac{m^* \rho}{r^{*2}} \left(1 + \frac{P}{\rho} \right) \left(1 + \frac{4\pi r^{*3} P}{m^*} \right) \left(1 - \frac{2m^*}{r^*} \right)^{-1}, \end{aligned} \quad (16)$$

where m^* , \bar{m}_b^* , P , ρ and ϵ_b are functions of r^* . For a given central density ρ_c and the EOS of the neutron star, solving Eq. (16) yields the quantities $\mathbf{M}^* = m^*(R^*)$ and $\bar{\mathbf{M}}^* = \bar{m}_b^*(R^*)$, where R^* is the stellar radius in the rescaled coordinates.

Now we define a function f which maps the value between the rescaled gravitational mass and baryon mass,

$$f : \mathbf{M}^* \mapsto \bar{\mathbf{M}}^*, \quad (17)$$

and its inverse map is denoted as g

$$g : \bar{\mathbf{M}}^* \mapsto \mathbf{M}^*. \quad (18)$$

For a neutron star with mass \mathbf{M} and the gravitational constant G , then we have $\mathbf{M}^* = G^{3/2} \mathbf{M}$, and $\bar{\mathbf{M}}^* = f(\mathbf{M}^*) = f(G^{3/2} \mathbf{M})$. The baryon mass for this neutron star is

$$\bar{\mathbf{M}} = G^{-3/2} \bar{\mathbf{M}}^* = G^{-3/2} f(G^{3/2} \mathbf{M}). \quad (19)$$

When the gravitational constant changes to $G_1 = G + \delta G$, the baryon mass keep fixed, and correspondingly, $\bar{\mathbf{M}}_1^* = G_1^{3/2} G^{-3/2} f(G^{3/2} \mathbf{M})$. Thus we have $\mathbf{M}_1^* = g(G_1^{3/2} G^{-3/2} f(G^{3/2} \mathbf{M}))$. So the mass of the neutron star changes to

$$\mathbf{M}_1 = G_1^{-3/2} g \left(G_1^{3/2} G^{-3/2} f(G^{3/2} \mathbf{M}) \right). \quad (20)$$

Hence the sensitivity can be expressed as

$$s = -\frac{G}{\mathbf{M}} \lim_{\delta G \rightarrow 0} \frac{\mathbf{M}_1 - \mathbf{M}}{\delta G} = \frac{3}{2} \left(1 - \frac{1}{G^{3/2} \mathbf{M}} f(G^{3/2} \mathbf{M}) g' \left(f(G^{3/2} \mathbf{M}) \right) \right), \quad (21)$$

where the prime denotes the derivative on G .

We can see that for a given EOS, the sensitivity depends on $G^{3/2} \mathbf{M}$. To obtain the numerical results of the sensitivities, we first solve Eq (14) with the current gravitational constant G_0 and with different initial values ρ_c to obtain $M(\rho_c)$ and $\bar{M}(\rho_c)$. Then we perform interpolation on the different data points $(\mathbf{M}(\rho_c), \bar{\mathbf{M}}(\rho_c))$ to obtain the function f and g' , and finally we use Eq. (21) with their variables \mathbf{M} replaced with $(G/G_0)^{3/2} \mathbf{M}$ to evaluate the sensitivities at different values of G . The resulting sensitivities for several representative EOSs are shown in Fig. 2. We find that the empirical relation in Eq. (13) provides a reasonable approximation at low masses, while for all EOSs considered the sensitivity increases monotonically with mass but remains below 1/2. This behavior reflects the fact that the sensitivity of a black hole is exactly 1/2, as discussed in the following for the cases of Schwarzschild and Reissner-Nordström (RN) black holes.

Sensitivities for black holes

Previous GW-based studies of varying- G theories have adopted a black-hole sensitivity of $s = 1/2$ [32, 35]. This value is well motivated by earlier work in scalar–tensor theories: in the Brans–Dicke formulation, *Will and Zaglauer* argued that the sensitivity of a stationary black hole equal 1/2 [40]. This value arises from the requirement imposed by Hawking’s theorem [41], which states that a stationary black hole in Brans–Dicke theory cannot support nontrivial scalar field configurations. Consequently, the scalar field must remain constant in any local freely falling frame, implying a vanishing post-Newtonian scalar-field expansion and leading to $s = 1/2$. Here we provide a complementary, model-independent argument demonstrating that the sensitivity of spherically symmetric black holes in varying- G theories is universally equal to 1/2.

The Einstein-Hilbert action is

$$S = \int \frac{R}{16\pi G} dx^4. \quad (22)$$

Under a varying G , the variation of the above action yields the equation of motion for the metric as

$$R_{\mu\nu} - \frac{1}{2} g_{\mu\nu} R - \frac{2(\nabla_\mu G)(\nabla_\nu G)}{G^2} + \frac{\nabla_\nu \nabla_\mu G}{G} - \frac{g_{\mu\nu}(\nabla_\rho \nabla^\rho G)}{G} + \frac{2g_{\mu\nu}(\nabla_\rho G)(\nabla^\rho G)}{G^2} = 0. \quad (23)$$

This equation is applicable not only to a varying- G with explicit time dependence, but also to a completely general varying- G that depends on the spacetime coordinates. Performing the trace-reversal of the equation, we obtain

$$R_{\mu\nu} - \frac{2(\nabla_\mu G)(\nabla_\nu G)}{G^2} + \frac{\nabla_\nu \nabla_\mu G}{G} + \frac{g_{\mu\nu}(\nabla_\rho \nabla^\rho G)}{2G} - \frac{g_{\mu\nu}(\nabla_\rho G)(\nabla^\rho G)}{G^2} = 0. \quad (24)$$

Now we consider a scenario in which the gravitational constant varies slowly with time, denoted by $G(t)$, and retain only leading-order contributions in time derivatives. At each time slice, the spherically symmetric vacuum solution can be approximated by the Schwarzschild black hole, hence the metric can be expressed as

$$g_{\mu\nu} = \text{diag} \left(-f(r, t), f(r, t)^{-1}, r^2, r^2 \sin(\theta)^2 \right), \quad (25)$$

where $f(r, t) = 1 - R_s(t)/r$ and $R_s(t) = 2G(t)M(t)$. Substituting the metric into Eq. (24), the (0, 1) component of the field equations yields

$$R_s(t)G'(t) - 2G(t)R'_s(t) = 0, \quad (26)$$

where the prime represents the derivative on time. Then we have,

$$R_s(t) \propto \sqrt{G(t)}. \quad (27)$$

Substituting the result into the field equation, we can see that other components are zero up to leading order. It follows that the black-hole mass evolves as

$$M(t) \propto \frac{R_s(t)}{G(t)} = G(t)^{-\frac{1}{2}}, \quad (28)$$

and therefore the sensitivity is

$$s = -\frac{\partial \ln M}{\partial \ln G} = \frac{1}{2}. \quad (29)$$

The same reasoning applies to charged black holes. For a RN black hole we adopt the metric function

$$f(r, t) = 1 - \frac{R_m(r)}{r} + \frac{4\pi G(t)Q(t)}{r^2}, \quad (30)$$

together with the electromagnetic four-potential

$$A_\mu = \left(\frac{Q(t)}{r^2}, 0, 0, 0 \right). \quad (31)$$

Assuming a slowly varying gravitational constant, we expand

$$\begin{aligned} G(t) &= G_0(1 + \lambda t) + O(t)^2, \\ R_m(t) &= R_0(1 + \alpha \lambda t) + O(t)^2, \\ Q(t) &= Q_0(1 + \beta \lambda t) + O(t)^2. \end{aligned} \quad (32)$$

Substituting these expressions into the field equations and retaining leading-order terms, we find

$$\alpha = \frac{1}{2}, \quad \beta = 0, \quad (33)$$

which shows that $s = 1/2$ and the electric charge does not vary with time in varying- G theories, as it naturally should not.

GW propagating in varying- G FLRW universe

In many GW tests of modified gravity, propagation effects are frequently overlooked. However, if the gravitational coupling varies with cosmic time, the evolution of G during GW propagation can lead to observable modifications to the waveform amplitude. In particular, Refs. [33, 34] showed that, in varying- G theories, the GW amplitude acquires a correction factor of $\sqrt{G_0/G_*}$, where G_* and G_0 denote the gravitational constant at the source and at the detector, respectively. That result was derived from a perturbative expansion around Minkowski spacetime. Here we demonstrate that the same amplitude correction persists for GW propagation in a FLRW universe.

We consider the physical metric $\tilde{g}_{\mu\nu}$ as a perturbation around a homogeneous and isotropic FLRW background,

$$\tilde{g}_{\mu\nu} = g_{\mu\nu} + h_{\mu\nu}, \quad (34)$$

where $g_{\mu\nu} = \text{diag}(-a^2(\eta), a^2(\eta), a^2(\eta), a^2(\eta))$ is the background FLRW metric in the comoving coordinate (η, x, y, z) , $a(\eta)$ is the scale factor, and $h_{\mu\nu}$ denotes the metric perturbation. Expanding the field equations (24) to linear order in $h_{\mu\nu}$, we obtain

$$\begin{aligned} 0 = & -\frac{1}{2}\nabla_\nu\nabla_\mu h^\rho{}_\rho + \frac{1}{2}\nabla_\rho\nabla_\mu h_\nu{}^\rho + \frac{1}{2}\nabla_\rho\nabla_\nu h_\mu{}^\rho - \frac{1}{2}\nabla_\rho\nabla^\rho h_{\mu\nu} + \frac{h_{\mu\nu}\nabla_\rho\nabla^\rho G}{2G} - \frac{\nabla_\mu h_{\nu\rho}\nabla^\rho G}{2G} - \frac{\nabla_\nu h_{\mu\rho}\nabla^\rho G}{2G} \\ & + \frac{\nabla_\rho h_{\mu\nu}\nabla^\rho G}{2G} + \frac{g_{\mu\nu}\nabla_\rho h^\sigma{}_\sigma\nabla^\rho G}{4G} - \frac{h_{\mu\nu}\nabla_\rho G\nabla^\rho G}{G^2} - \frac{g_{\mu\nu}\nabla^\rho G\nabla_\sigma h_\rho{}^\sigma}{2G} + \frac{h_{\rho\sigma}g_{\mu\nu}\nabla^\rho G\nabla^\sigma G}{G^2} - \frac{h_{\rho\sigma}g_{\mu\nu}\nabla^\sigma\nabla^\rho G}{2G}, \end{aligned} \quad (35)$$

where the covariant derivative is defined with respect to the background metric $g_{\mu\nu}$. For simplicity, we consider a GW propagating along the z -direction and work in the transverse-traceless gauge. The nonvanishing components of the metric perturbation are

$$\begin{aligned} h_{11} &= -h_{22} = a(\eta)h_+(\eta, z), \\ h_{12} &= h_{21} = a(\eta)h_\times(\eta, z), \end{aligned} \quad (36)$$

with other components to be zero. Substitute this ansatz into into Eq. (35), we find that the (1, 1), (1, 2), (2, 1) and (2, 2) components yield identical equations for the two GW polarizations h_+ and h_\times ,

$$\partial_\eta^2 h_{+/\times} + \left(\frac{2a'}{a} - \frac{G'}{G} \right) \partial_\eta h_{+/\times} - \partial_z^2 h_{+/\times} + \left(\frac{2a''}{a} + \frac{2a'^2}{a^2} - \frac{4a'G'}{aG} - \frac{G''}{G} + \frac{2G'^2}{G^2} \right) h_{+/\times} = 0, \quad (37)$$

where primes denote derivatives with respect to conformal time η . Assuming a plane-wave solution $h(\eta, z) = A(\eta)e^{ikz}$, the amplitude $A(\eta)$ satisfies

$$A'' + \left(\frac{2a'}{a} - \frac{G'}{G} \right) A' + \left(k^2 + \frac{2a''}{a} + \frac{2a'^2}{a^2} - \frac{4a'G'}{aG} - \frac{G''}{G} + \frac{2G'^2}{G^2} \right) A = 0. \quad (38)$$

Introducing the redefinition $A(\eta) = B(\eta)\frac{\sqrt{G(\eta)}}{a(\eta)}$, the above equation reduces to

$$B'' + \left(k^2 + \frac{a''}{a} + \frac{2a'^2}{a^2} - \frac{3a'G'}{aG} - \frac{G''}{2G} + \frac{5G'^2}{4G^2} \right) B = 0. \quad (39)$$

For GWs with wavelengths much shorter than the Hubble radius, all terms in the brackets except k^2 are negligible, yielding $B'' + k^2 B = 0$. The resulting GW solution is therefore

$$h = \frac{\sqrt{G(\eta)}}{a(\eta)} \exp(ik(z \pm \eta)). \quad (40)$$

Denoting the GW amplitudes at the source and observer by A_s and A_{obs} , we have the relation $A_s a(\eta_s) / \sqrt{G_*} = A_{\text{obs}} a(\eta_o) / \sqrt{G_0}$, so we have

$$A_{\text{obs}} = \frac{a(\eta_s)}{a(\eta_o)} \sqrt{\frac{G_0}{G_*}} A_s. \quad (41)$$

The coefficient related to $a(\eta)$ corresponds to the standard cosmological redshift effect and is absorbed into the definition of the luminosity distance D_L . The additional factor $\sqrt{G_0/G_*}$ represents a genuine propagation effect induced by the variation of the gravitational constant, in agreement with previous results obtained in Minkowski spacetime [33, 34].

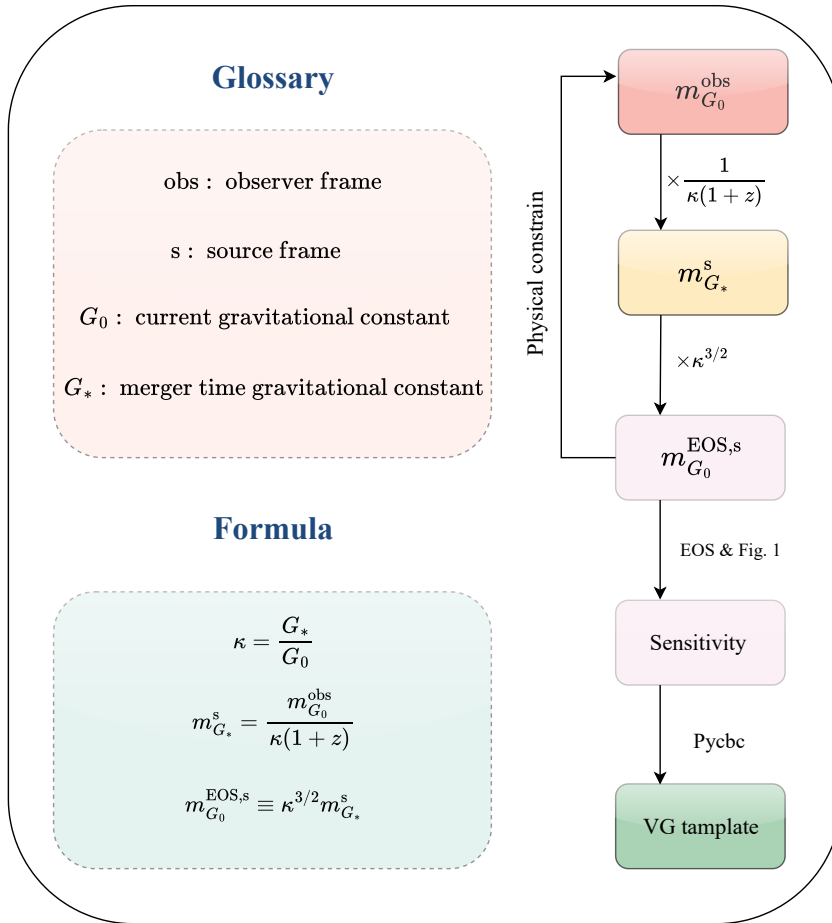


Fig. 3 Workflow for constructing GW waveform templates in a varying- G theory.

Bayesian inference of varying- G theory

In this section, we provide a detailed description of the varying- G waveform template construction procedures and the corresponding Bayesian inference settings.

Varying- G waveform template

Under the assumption that the gravitational constant varies slowly on cosmological timescales, its time dependence can be treated as linear at leading order [21, 28]. The variation of the gravitational constant between the source and the detector can therefore be parametrized by

$$\kappa \equiv \frac{G_*}{G_0}, \quad (42)$$

denote the values of the gravitational constant at the source and at the detector, respectively. The corresponding fractional time derivative is related to κ by

$$\frac{\dot{G}}{G} = \frac{G_0 - G_*}{G_0 T} = \frac{1 - \kappa}{T}, \quad (43)$$

where T is the lookback time from the merger epoch to the present. In our numerical implementation and Bayesian inference, we adopt κ as the fundamental parameter characterizing varying- G effects, and convert it to \dot{G}/G when presenting the final constraints.

In the GR scenario, the GW waveforms depend on the dimensionless combination GMf/c^3 , and the LALSImulation [42, 43] adopts natural units with $G = c = 1$. Because of cosmological redshift, GW data analysis distinguishes between the source frame and the detector frame, related by

$$M_s = \frac{M_{\text{obs}}}{1+z}, \quad (44)$$

$$f_s = f_{\text{obs}}(1+z), \quad (45)$$

where z is the redshift and subscripts “s” and “obs” denote the source and detector frames, respectively.

In the varying- G scenario, analogous to the distinction between the source frame and the detector frame in GR, we define corresponding frames. Denoting the source-frame parameters by $\{G_*, m_{G_*}^s, f_s\}$ and the detector-frame parameters by $\{G_0, m_{G_0}^{\text{obs}}, f_{\text{obs}}\}$, the invariance of the dimensionless combination implies

$$G_0 m_{G_0}^{\text{obs}} f_{\text{obs}} / c^3 = G_* m_{G_*}^s f_s / c^3, \quad (46)$$

$$f_{\text{obs}} = \frac{f_s}{1+z}, \quad (47)$$

which yields

$$m_{G_*}^s = \frac{G_0}{G_*} \frac{m_{G_0}^{\text{obs}}}{1+z} = \frac{m_{G_0}^{\text{obs}}}{\kappa(1+z)}. \quad (48)$$

Here $m_{G_0}^{\text{obs}}$ is an auxiliary mass parameter, defined in the detector frame for numerical convenience, and serves as an output of the program with no direct physical meaning. Conversely, $m_{G_*}^s$ is the true physical mass of the compact object at the source.

As shown in Sec. 4, the sensitivity of a neutron star depends on the combination $(G_*/G_0)^{3/2} m_{G_*}^s = \kappa^{3/2} m_{G_*}^s$. We therefore define the corresponding EOS mass under the present gravitational constant G_0 as

$$m_{G_0}^{\text{EOS},s} \equiv \kappa^{3/2} m_{G_*}^s = \frac{\kappa^{1/2}}{1+z} m_{G_0}^{\text{obs}}. \quad (49)$$

Following Ref. [30], this quantity must lie within the physically allowed mass range determined by the neutron-star EOS evaluated at G_0 . In this work, we adopt the widely used H4 EOS, which imposes the constraint

$$m_{G_0}^{\text{EOS},s} \in (0.08, 2.01) M_{\odot}, \quad (50)$$

as illustrated in Fig. 2.

When matching waveform templates to GW data, the phase evolution plays the dominant role in parameter estimation, while amplitude corrections are often subleading. In our analysis, the ppE amplitude correction au^a is found to be of order 10^{-16} across the Monte Carlo samples and is therefore entirely negligible. By contrast, the propagation effect induced by a varying gravitational constant introduces an amplitude correction factor of $1/\sqrt{\kappa}$, which must be retained.

Combining the ppE phase correction with the propagation effect, the detector-frame GW waveform template in the varying- G scenario is given by

$$\tilde{h}_{\text{VG}}(f) = \frac{1}{\sqrt{\kappa}} \tilde{h}_{\text{GR}} e^{i\beta_{\text{VG}} t^{b_{\text{VG}}}}, \quad (51)$$

where \tilde{h}_{GR} is the GR waveform template generated by PyCBC using the detector-frame mass $m_{G_0}^{\text{obs}}$, and

$$b_{\text{VG}} = -13,$$

$$\begin{aligned}\beta_{\text{VG}} &= -\frac{25}{851968}\eta^{3/5}\frac{1-\kappa}{T}G_*[(11+3(s_1+s_2))M_{G_*}^s - 41(m_{G_{*,1}}^s s_1 + m_{G_{*,2}}^s s_2)] \\ &= -\frac{25}{851968}\eta^{3/5}\frac{1-\kappa}{T(1+z)}G_0[(11+3(s_1+s_2))M_{G_0}^{\text{obs}} - 41(m_{G_{0,1}}^{\text{obs}} s_1 + m_{G_{0,2}}^{\text{obs}} s_2)],\end{aligned}$$

with s_1 and s_2 evaluated using the EOS masses $m_{G_{0,1}}^{\text{EOS},s}$ and $m_{G_{0,2}}^{\text{EOS},s}$, respectively. The overall workflow of the varying- G waveform construction is summarized in Fig. 3.

Table 1 Prior distributions used in the varying- G analysis of GW170817 with the TaylorF2 and IMRPhenomXAS_NRTidalv2 waveform templates.

Parameters	TaylorF2 (GR)	TaylorF2 (VG)	IMRPhenomXAS_NRTidalv2 (GR)	IMRPhenomXAS_NRTidalv2 (VG)
\mathcal{M}_c [M_\odot]	$\mathcal{U}[1.15, 1.23]$	$\mathcal{U}[1.15, 1.23]$	$\mathcal{U}[1.15, 1.23]$	$\mathcal{U}[1.15, 1.23]$
q	$\mathcal{U}[1.00, 2.00]$	$\mathcal{U}[1.00, 2.00]$	$\mathcal{U}[1.00, 2.00]$	$\mathcal{U}[1.00, 2.00]$
χ_{1z}	$\mathcal{U}[-0.05, 0.05]$	$\mathcal{U}[-0.05, 0.05]$	$\mathcal{U}[-0.05, 0.05]$	$\mathcal{U}[-0.05, 0.05]$
χ_{2z}	$\mathcal{U}[-0.05, 0.05]$	$\mathcal{U}[-0.05, 0.05]$	$\mathcal{U}[-0.05, 0.05]$	$\mathcal{U}[-0.05, 0.05]$
Λ_1	$\mathcal{U}[0, 5000]$	$\mathcal{U}[0, 5000]$	$\mathcal{U}[0, 5000]$	$\mathcal{U}[0, 5000]$
Λ_2	$\mathcal{U}[0, 5000]$	$\mathcal{U}[0, 5000]$	$\mathcal{U}[0, 5000]$	$\mathcal{U}[0, 5000]$
κ	–	Log uniform [$10^{-4}, 100$]	–	Log uniform [$10^{-4}, 100$]
D_L [Mpc]	40.7	40.7	40.7	40.7
ι [rad]	sine uniform	$\mathcal{U}[2.70, 2.81]$	sine uniform	$\mathcal{U}[2.70, 2.81]$
α [rad]	3.45	3.45	3.45	3.45
δ [rad]	-0.41	-0.41	-0.41	-0.41
ψ [rad]	$\mathcal{U}[0, 2\pi]$	$\mathcal{U}[0, 2\pi]$	$\mathcal{U}[0, 2\pi]$	$\mathcal{U}[0, 2\pi]$
δt_c [s]	$\mathcal{U}[-0.1, 0.1]$	$\mathcal{U}[-0.1, 0.1]$	$\mathcal{U}[-0.1, 0.1]$	$\mathcal{U}[-0.1, 0.1]$
ϕ_c [rad]	$\mathcal{U}[0, 2\pi]$	$\mathcal{U}[0, 2\pi]$	$\mathcal{U}[0, 2\pi]$	$\mathcal{U}[0, 2\pi]$

Bayesian inference

In this work, we inference both GR and non-GR parameters from the observed GW data within a Bayesian framework [44]. The posterior distribution of model parameters ϑ , given the observed data d and hypothesis \mathcal{H} is,

$$p(\vartheta|d, \mathcal{H}) = \frac{p(d|\vartheta, \mathcal{H}) p(\vartheta|\mathcal{H})}{p(d|\mathcal{H})}, \quad (52)$$

where $p(d|\vartheta, \mathcal{H})$ is the likelihood, $p(\vartheta|\mathcal{H})$ the prior, and $p(d|\mathcal{H})$ the Bayesian evidence.

For a network of multiple detectors, assuming stationary Gaussian noise, the log-likelihood takes the form

$$\log p(d|\vartheta, \mathcal{H}) = \log \bar{\alpha} - \frac{1}{2} \sum_i \langle d_i - h_i(\vartheta) | d_i - h_i(\vartheta) \rangle, \quad (53)$$

where $\log \bar{\alpha}$ is the normalizing constant, the index i labels individual detectors, and $h_i(\vartheta)$ denotes the waveform template projected onto the i -th detector. The inner product is defined as,

$$\langle a(t) | b(t) \rangle = 2 \int_{f_{\text{low}}}^{f_{\text{high}}} \frac{\tilde{a}^*(f) \tilde{b}(f) + \tilde{a}(f) \tilde{b}^*(f)}{S_n(f)} df. \quad (54)$$

where $S_n(f)$ is the one-sided noise power spectral density, and f_{low} and f_{high} denote the lower and upper frequency cutoffs of the analysis, respectively.

We consider the spin aligned BNS systems including tidal interactions. In this case, the GR waveform is described by the following set of 13 parameters:

$$\vartheta_{\text{GR}} = \{\mathcal{M}_c, q, \chi_{1z}, \chi_{2z}, \Lambda_1, \Lambda_2, D_L, \iota, \alpha, \delta, \psi, t_c, \phi_c\}, \quad (55)$$

where \mathcal{M}_c and q are chirp mass and mass ratio, χ_{1z} and χ_{2z} are the dimensionless spin components aligned with the orbital angular momentum, Λ_1 and Λ_2 are the tidal deformabilities, D_L is the luminosity distance, α and δ are the right ascension

and declination angles, ι and ψ denote the inclination angle the polarization angle, and ϕ_c and t_c are the coalescence phase and time, respectively.

In the varying- G framework, an additional non-GR parameter κ is introduced, such that

$$\vartheta_{\text{VG}} = \vartheta_{\text{GR}} + \{\kappa\}. \quad (56)$$

We apply this framework to GW170817, the first observed BNS inspiral and the first gravitational-wave event with confirmed electromagnetic counterparts. Follow-up electromagnetic observations provide precise and independent constraints on several extrinsic parameters of the source. To improve the efficiency and robustness of the Bayesian inference, we fix the luminosity distance to $D_L = 40.7$ Mpc, inferred from surface brightness fluctuation measurement with the Hubble Space Telescope [17], corresponding to a lookback time of $T = 1.31 \times 10^8$ years. We further fix the sky location to $\alpha = 3.45$ rad and $\delta = -0.41$ rad based on observations with the Dark Energy Camera [16]. As a result, 10 and 11 parameters remain to be sampled in the GR and varying- G , respectively.

As shown in Eq. (51), the propagation effect induced by a varying gravitational constant introduces a multiplicative correction to the waveform amplitude, giving rise to degeneracies between the non-GR parameter κ and both the luminosity distance D_L and the inclination angle ι . In this analysis, the degeneracy between κ and D_L is removed by fixing D_L using independent electromagnetic distance measurements. A remaining degeneracy between κ and ι therefore needs to be broken. To this end, we incorporate independent constraints on the inclination obtained from very long baseline interferometry (VLBI) observations of the GW170817 afterglow. These measurements constrain the inclination to the 90% credible interval [2.70, 2.81] rad [18–20]. We adopt this interval as the prior on ι in the varying- G analysis, while a sine-uniform prior is used in the GR case. The complete prior distributions employed in both analyses are summarized in Table 1.

Acknowledgements.— This work is supported in part by National Natural Science Foundation of China under Grant No. 12335006 and in part by the National Natural Science Foundation of China under Grant No. 12547101. ZL is supported by “the Fundamental Research Funds for the Central Universities”. It is also supported by the High-performance Computing Platform of Peking University.

References

- [1] Ghez, A.M., Salim, S., Hornstein, S.D., Tanner, A., Morris, M., Becklin, E.E., Duchene, G.: Stellar orbits around the galactic center black hole. *Astrophys. J.* **620**, 744–757 (2005) <https://doi.org/10.1086/427175> [arXiv:astro-ph/0306130](https://arxiv.org/abs/astro-ph/0306130)
- [2] Psaltis, D.: Probes and Tests of Strong-Field Gravity with Observations in the Electromagnetic Spectrum. *Living Rev. Rel.* **11**, 9 (2008) <https://doi.org/10.12942/lrr-2008-9> [arXiv:0806.1531](https://arxiv.org/abs/0806.1531) [astro-ph]
- [3] Will, C.M.: The Confrontation between General Relativity and Experiment. *Living Rev. Rel.* **17**, 4 (2014) <https://doi.org/10.12942/lrr-2014-4> [arXiv:1403.7377](https://arxiv.org/abs/1403.7377) [gr-qc]
- [4] Freire, P.C.C., Wex, N.: Gravity experiments with radio pulsars. *Living Rev. Rel.* **27**(1), 5 (2024) <https://doi.org/10.1007/s41114-024-00051-y> [arXiv:2407.16540](https://arxiv.org/abs/2407.16540) [gr-qc]
- [5] Williams, J.G., Turyshev, S.G., Boggs, D.H.: Progress in lunar laser ranging tests of relativistic gravity. *Phys. Rev. Lett.* **93**, 261101 (2004) <https://doi.org/10.1103/PhysRevLett.93.261101> [arXiv:gr-qc/0411113](https://arxiv.org/abs/gr-qc/0411113)
- [6] Hofmann, F., Müller, J.: Relativistic tests with lunar laser ranging. *Class. Quant. Grav.* **35**(3), 035015 (2018) <https://doi.org/10.1088/1361-6382/aa8f7a>
- [7] Kaspi, V.M., Taylor, J.H., Ryba, M.F.: High - precision timing of millisecond pulsars. 3: Long - term monitoring of PSRs B1855+09 and B1937+21. *Astrophys. J.* **428**, 713 (1994) <https://doi.org/10.1086/174280>
- [8] Thorsett, S.E.: The Gravitational constant, the Chandrasekhar limit, and neutron star masses. *Phys. Rev. Lett.* **77**, 1432–1435 (1996) <https://doi.org/10.1103/PhysRevLett.77.1432> [arXiv:astro-ph/9607003](https://arxiv.org/abs/astro-ph/9607003)
- [9] Deller, A.T., Verbiest, J.P.W., Tingay, S.J., Bailes, M.: Extremely high precision VLBI astrometry of PSR J0437-4715 and implications for theories of gravity. *Astrophys. J. Lett.* **685**, 67 (2008) <https://doi.org/10.1086/592401> [arXiv:0808.1594](https://arxiv.org/abs/0808.1594) [astro-ph]
- [10] Zhu, W.W., *et al.*: Testing Theories of Gravitation Using 21-Year Timing of Pulsar Binary J1713+0747. *Astrophys. J.* **809**(1), 41 (2015) <https://doi.org/10.1088/0004-637X/809/1/41> [arXiv:1504.00662](https://arxiv.org/abs/1504.00662) [astro-ph.SR]

- [11] Zhu, W.W., *et al.*: Tests of Gravitational Symmetries with Pulsar Binary J1713+0747. *Mon. Not. Roy. Astron. Soc.* **482**(3), 3249–3260 (2019) <https://doi.org/10.1093/mnras/sty2905> arXiv:1802.09206 [astro-ph.HE]
- [12] Wu, F., Chen, X.: Cosmic microwave background with Brans-Dicke gravity II: constraints with the WMAP and SDSS data. *Phys. Rev. D* **82**, 083003 (2010) <https://doi.org/10.1103/PhysRevD.82.083003> arXiv:0903.0385 [astro-ph.CO]
- [13] Abbott, B.P., *et al.*: GW170817: Observation of Gravitational Waves from a Binary Neutron Star Inspiral. *Phys. Rev. Lett.* **119**(16), 161101 (2017) <https://doi.org/10.1103/PhysRevLett.119.161101> arXiv:1710.05832 [gr-qc]
- [14] Abbott, B.P., *et al.*: Gravitational Waves and Gamma-rays from a Binary Neutron Star Merger: GW170817 and GRB 170817A. *Astrophys. J. Lett.* **848**(2), 13 (2017) <https://doi.org/10.3847/2041-8213/aa920c> arXiv:1710.05834 [astro-ph.HE]
- [15] Abbott, B.P., *et al.*: Multi-messenger Observations of a Binary Neutron Star Merger. *Astrophys. J. Lett.* **848**(2), 12 (2017) <https://doi.org/10.3847/2041-8213/aa91c9> arXiv:1710.05833 [astro-ph.HE]
- [16] Soares-Santos, M., *et al.*: The Electromagnetic Counterpart of the Binary Neutron Star Merger LIGO/Virgo GW170817. I. Discovery of the Optical Counterpart Using the Dark Energy Camera. *Astrophys. J. Lett.* **848**(2), 16 (2017) <https://doi.org/10.3847/2041-8213/aa9059> arXiv:1710.05459 [astro-ph.HE]
- [17] Cantiello, M., *et al.*: A Precise Distance to the Host Galaxy of the Binary Neutron Star Merger GW170817 Using Surface Brightness Fluctuations. *Astrophys. J. Lett.* **854**(2), 31 (2018) <https://doi.org/10.3847/2041-8213/aaad64> arXiv:1801.06080 [astro-ph.GA]
- [18] Mooley, K.P., *et al.*: A mildly relativistic wide-angle outflow in the neutron star merger GW170817. *Nature* **554**, 207 (2018) <https://doi.org/10.1038/nature25452> arXiv:1711.11573 [astro-ph.HE]
- [19] Mooley, K.P., Deller, A.T., Gottlieb, O., Nakar, E., Hallinan, G., Bourke, S., Frail, D.A., Horesh, A., Corsi, A., Hotokezaka, K.: Superluminal motion of a relativistic jet in the neutron-star merger GW170817. *Nature* **561**(7723), 355–359 (2018) <https://doi.org/10.1038/s41586-018-0486-3> arXiv:1806.09693 [astro-ph.HE]
- [20] Mooley, K.P., Anderson, J., Lu, W.: Optical superluminal motion measurement in the neutron-star merger GW170817. *Nature* **610**(7931), 273–276 (2022) <https://doi.org/10.1038/s41586-022-05145-7> arXiv:2210.06568 [astro-ph.HE]
- [21] Nordtvedt, K.: \dot{G}/G and a cosmological acceleration of gravitationally compact bodies. *Phys. Rev. Lett.* **65**, 953–956 (1990) <https://doi.org/10.1103/PhysRevLett.65.953>
- [22] LIGO Scientific Collaboration and Virgo Collaboration: The Gravitational-wave Transient Catalog. <https://gwosc.org/eventapi/html/GWTC/> (2025)
- [23] Biwer, C.M., Capano, C.D., De, S., Cabero, M., Brown, D.A., Nitz, A.H., Raymond, V.: PyCBC Inference: A Python-based parameter estimation toolkit for compact binary coalescence signals. *Publ. Astron. Soc. Pac.* **131**(996), 024503 (2019) <https://doi.org/10.1088/1538-3873/aaef0b> arXiv:1807.10312 [astro-ph.IM]
- [24] Bonilla, G.S., Kumar, P., Teukolsky, S.A.: Modeling compact binary merger waveforms beyond general relativity. *Phys. Rev. D* **107**(2), 024015 (2023) <https://doi.org/10.1103/PhysRevD.107.024015> arXiv:2203.14026 [gr-qc]
- [25] Song, H., Li, H., Lyu, Z., Zhu, J., Wang, J.-C., Ji, P.: Constraining noncommutative spacetime with GW150914 and GW190814 (2025) arXiv:2507.23442 [gr-qc]
- [26] Nitz, A.H., Kumar, S., Wang, Y.-F., Kasta, S., Wu, S., Schäfer, M., Dhurkunde, R., Capano, C.D.: 4-OGC: Catalog of Gravitational Waves from Compact Binary Mergers. *Astrophys. J.* **946**(2), 59 (2023) <https://doi.org/10.3847/1538-4357/aca591> arXiv:2112.06878 [astro-ph.HE]
- [27] Chamberlain, K., Yunes, N.: Theoretical Physics Implications of Gravitational Wave Observation with Future Detectors. *Phys. Rev. D* **96**(8), 084039 (2017) <https://doi.org/10.1103/PhysRevD.96.084039> arXiv:1704.08268 [gr-qc]
- [28] Tahura, S., Yagi, K.: Parameterized Post-Einsteinian Gravitational Waveforms in Various Modified Theories of Gravity. *Phys. Rev. D* **98**(8), 084042 (2018) <https://doi.org/10.1103/PhysRevD.98.084042> arXiv:1809.00259 [gr-qc]. [Erratum: *Phys.Rev.D* 101, 109902 (2020)]

- [29] Tahura, S., Yagi, K., Carson, Z.: Testing Gravity with Gravitational Waves from Binary Black Hole Mergers: Contributions from Amplitude Corrections. *Phys. Rev. D* **100**(10), 104001 (2019) <https://doi.org/10.1103/PhysRevD.100.104001> [arXiv:1907.10059](https://arxiv.org/abs/1907.10059) [gr-qc]
- [30] Vijaykumar, A., Kapadia, S.J., Ajith, P.: Constraints on the time variation of the gravitational constant using gravitational-wave observations of binary neutron stars. *Phys. Rev. Lett.* **126**(14), 141104 (2021) <https://doi.org/10.1103/PhysRevLett.126.141104> [arXiv:2003.12832](https://arxiv.org/abs/2003.12832) [gr-qc]
- [31] Barbieri, R., Savastano, S., Speri, L., Antonelli, A., Sberna, L., Burke, O., Gair, J., Tamanini, N.: Constraining the evolution of Newton's constant with slow inspirals observed from spaceborne gravitational-wave detectors. *Phys. Rev. D* **107**(6), 064073 (2023) <https://doi.org/10.1103/PhysRevD.107.064073> [arXiv:2207.10674](https://arxiv.org/abs/2207.10674) [gr-qc]
- [32] Wang, Z., Zhao, J., An, Z., Shao, L., Cao, Z.: Simultaneous bounds on the gravitational dipole radiation and varying gravitational constant from compact binary inspirals. *Phys. Lett. B* **834**, 137416 (2022) <https://doi.org/10.1016/j.physletb.2022.137416> [arXiv:2208.11913](https://arxiv.org/abs/2208.11913) [gr-qc]
- [33] An, J., Xue, Y., Cao, Z., He, X., Sun, B.: The effect of the gravitational constant variation on the propagation of gravitational waves. *Phys. Lett. B* **844**, 138108 (2023) <https://doi.org/10.1016/j.physletb.2023.138108> [arXiv:2307.15382](https://arxiv.org/abs/2307.15382) [gr-qc]
- [34] Sun, B., An, J., Cao, Z.: Constrain the time variation of the gravitational constant via the propagation of gravitational waves. *Phys. Lett. B* **848**, 138350 (2024) <https://doi.org/10.1016/j.physletb.2023.138350> [arXiv:2308.00233](https://arxiv.org/abs/2308.00233) [gr-qc]
- [35] Yuan, X., Zhang, J.-d., Mei, J.: Distinguishing the environmental effects and modified theory of gravity with multiple massive black-hole binaries. *Phys. Rev. D* **111**(10), 104050 (2025) <https://doi.org/10.1103/PhysRevD.111.104050> [arXiv:2412.00915](https://arxiv.org/abs/2412.00915) [gr-qc]
- [36] An, J., Sun, B., Cao, Z.: The effect of the gravitational constant variation on the phase of gravitational waves. *Phys. Dark Univ.* **50**, 102062 (2025) <https://doi.org/10.1016/j.dark.2025.102062> [arXiv:2508.21746](https://arxiv.org/abs/2508.21746) [gr-qc]
- [37] Yunes:2009k, N., Yunes:2009k, F.: Fundamental Theoretical Bias in Gravitational Wave Astrophysics and the Parameterized Post-Einsteinian Framework. *Phys. Rev. D* **80**, 122003 (2009) <https://doi.org/10.1103/PhysRevD.80.122003> [arXiv:0909.3328](https://arxiv.org/abs/0909.3328) [gr-qc]
- [38] Lattimer, J.M.: Neutron star structure and the equation of state. *Prog. Theor. Phys. Suppl.* **186**, 1–8 (2010) <https://doi.org/10.1143/PTPS.186.1>
- [39] Lattimer, J.M., Prakash, M.: Neutron star structure and the equation of state. *Astrophys. J.* **550**, 426 (2001) <https://doi.org/10.1086/319702> [arXiv:astro-ph/0002232](https://arxiv.org/abs/astro-ph/0002232)
- [40] Will, C.M., Zaglauer, H.W.: Gravitational Radiation, Close Binary Systems, and the Brans-dicke Theory of Gravity. *Astrophys. J.* **346**, 366 (1989) <https://doi.org/10.1086/168016>
- [41] Hawking, S.W.: Black holes in the Brans-Dicke theory of gravitation. *Commun. Math. Phys.* **25**, 167–171 (1972) <https://doi.org/10.1007/BF01877518>
- [42] LIGO Scientific Collaboration, Virgo Collaboration, KAGRA Collaboration: LVK Algorithm Library - LALSuite. Free software (GPL) (2018). <https://doi.org/10.7935/GT1W-FZ16>
- [43] Wette, K.: SWIGLAL: Python and Octave interfaces to the LALSuite gravitational-wave data analysis libraries. *SoftwareX* **12**, 100634 (2020) <https://doi.org/10.1016/j.softx.2020.100634>
- [44] Finn, L.S.: Detection, measurement and gravitational radiation. *Phys. Rev. D* **46**, 5236–5249 (1992) <https://doi.org/10.1103/PhysRevD.46.5236> [arXiv:gr-qc/9209010](https://arxiv.org/abs/gr-qc/9209010)